UNIVERSITÀ POLITECNICA DELLE MARCHE
Repository ISTITUZIONALE

Nonlinear free dynamics of a two-layer composite beam with different boundary conditions

This is the peer reviewd version of the followng article:

Original
Nonlinear free dynamics of a two-layer composite beam with different boundary conditions / Lenci, S.; Clementi, F.; Warminski, J.. - In: MECCANICA. - ISSN 0025-6455. - STAMPA. - 50:3(2015), pp. 675-688. [10.1007/s11012-014-9945-6]

Availability:
This version is available at: 11566/169303 since: 2022-06-08T18:04:14Z

Publisher:

Published
DOI:10.1007/s11012-014-9945-6

Terms of use:

The terms and conditions for the reuse of this version of the manuscript are specified in the publishing policy. The use of copyrighted works requires the consent of the rights' holder (author or publisher). Works made available under a Creative Commons license or a Publisher's custom-made license can be used according to the terms and conditions contained therein. See editor's website for further information and terms and conditions.
This item was downloaded from IRIS Università Politecnica delle Marche (https://iris.univpm.it). When citing, please refer to the published version.

(Article begins on next page)

12 October 2024

Manuscript
Click here to download Manuscript: paper_revised.pdf
Click here to view linked References

Noname manuscript No.
(will be inserted by the editor)

Nonlinear free dynamics of a two-layer composite beam with different boundary conditions

Stefano Lenci · Francesco Clementi · Jerzy Warminski

Received: date / Accepted: date

Abstract The nonlinear free vibrations of a two-layer elastic composite beam are investigated. Different boundary conditions, both symmetric and not symmetric with respect to the beam midpoint, equal on both layers and different on each layers, are considered. The analysis is developed by means of the multiple time scale method, and at each order of the asymptotic development, we obtain different information. The first order terms provide the linear natural frequencies. The first, the second and the third natural frequencies are computed explicitly. The next order terms, on the other hand, provide the nonlinearity coefficients measuring the nonlinear amplitude dependence of the natural frequencies, i.e. the curvature of the backbone curve. Both the linear frequencies and the nonlinear coefficients are found to be dependent on two dimensionless parameters only and, for boundary conditions different on each layer, also of the ratio between the axial stiffnesses of each layer.

Keywords Two-layer beam · Nonlinear interface · Different boundary conditions · Free vibrations

S. Lenci
Dep. of Civil and Buildings Engineering, and Architecture
Polytechnic University of Marche, Ancona, Italy
Tel.: +39-071-2204552
Fax: +39-071-2204576
E-mail: lenci@univpm.it

F. Clementi
Dep. of Civil and Buildings Engineering, and Architecture
Polytechnic University of Marche, Ancona, Italy
E-mail: francesco.clementi@univpm.it

J. Warminski
Dep. of Applied Mechanics
Lublin University of Technology, Lublin, Poland
E-mail: j.warminski@pollub.pl

1 Introduction

This paper focus on the nonlinear dynamics of a two-layer composite beams. While a lot of investigations have been devoted to sandwich beams [1–6] where the distance between the layers (i.e., the interlayer thickness) is large, here we consider the case in which the thickness is small. This situation is commonly encountered in applications: structural glass, cross-ply laminated composite beams, steel-concrete beams, concrete / steel / wood beams reinforced with FRP sheet, etc. is a non-exhaustive list of examples.

The applications which are lurking in the background not only have a small thickness, but they also have an interlayer which is made by a material which is less stiff than the beams. In this situation, it may happen that the interlayer undergoes large deformations, still remaining in the nonlinear elastic regime, while the beams behave linearly. To give an idea of the nonlinear elastic behavior of the interface we note that Ivanov et al. [7] obtain $\tau = 0.5173\gamma + 0.0772\gamma^3$ (the shear stress τ is in [MPa]; γ is the shear strain) in static experiments of PVB, which is the interlayer mostly used in structural glass.

The dynamic behavior of two-layer beams, and of other composite beams [8,9], has been largely studied in the literature [10–17], where numerical [18,19], analytical/theoretical [20–22] as well as experimental [23, 24] studies can be found. To the best of authors' knowledge, the existing analyses focus on the geometric nonlinearities of the beams/plates, and not explicitly on the nonlinearity of the interlayer [7] (but see [25,26] in the dynamic case and [27] in the static case), which is instead the main assumption of this work. Indeed, in our model the unique nonlinearity is the nonlinear elastic behavior of the interlayer.

In this paper we extend to different boundary conditions (b.c.) the work reported in [25] where a two-layer composite free-free beam with nonlinear zero-thickness interface is considered. The beams have an Euler-Bernoulli kinematics and perfect adherence in the normal direction: only nonlinear elastic slipping is allowed at interface. The reliability of these hypotheses has been discussed in [16,17] where the full problem with shear deformations, axial and rotational inertia, and interface uplift is considered.

We pay attention to the effects of different b.c. on the linear and nonlinear frequencies of the two-layer beam. We consider both symmetric (e.g., free-free, fixed-fixed and hinged-hinged) and non-symmetric (e.g., free-fixed and hinged-fixed) b.c. We also consider the case of layers having different b.c., one fixed-fixed and the other free-free, which occurs for example in coating and in beams reinforced with FRP strips.

The free vibrations are studied by means of the multiple time scale method, which permits us to address the nonlinear problem analytically and provides an accurate estimation of the nonlinear, amplitude dependent, natural frequencies. The backbone curve is obtained, and the nonlinearity coefficient is found to be a function of two dimensionless parameters only, apart from the case in which the layers have different b.c. where it also depends on the ratio between the axial stiffnesses of the layers.

The paper is organized as follows. In Sect. 2 the governing equations are obtained by means of the Hamiltonian principle. Contrarily to [25], here we consider the three coupled equations and do not transform them in an equivalent higher order single equation. In Sect. 3 the multiple time scale method is applied, by directly selecting only the non-vanishing terms of the development and the non-vanishing slow times. In Sect. 4 the first order terms, which provided the linear natural frequencies, are obtained, while in Sect. 5 the third order terms, which provided the curvature of the backbone curve, i.e. the amplitude dependent correction of the linear frequencies, are obtained. Finally, the paper ends with some conclusions (Sect. 6).

2 Governing equations

In the considered two-layer composite each layer behaves like a linear elastic planar Euler-Bernoulli beam. The interface allows tangential slipping $S_T(Z,T)$ but guarantees perfect adherence in the transversal direction, so that the transversal displacement $V(Z,T)$ is unique, while each beam has its own axial displacement, $W_1(Z,T)$ and $W_2(Z,T)$, respectively. The mechanical behavior of the interface is nonlinear, i.e. the tangential force per unit length F_T is a nonlinear function of S_T. This is the unique source on nonlinearity. Finally, the axial and rotational inertia of both beams are neglected. This model has been previously investigated in [25], and this work constitutes a natural and announced continuation. According to the previous kinematic hypotheses, the strain, the kinetic and the potential energies are given by

$$E_s = \frac{1}{2}\int_0^L [EI(V'')^2 + \sum_{i=1}^{2} E_i A_i (W_i')^2]dZ + \int_0^L G(S_t)dZ,$$
$$E_k = \int_0^L \rho A \dot{V}^2 dZ, \qquad E_p = \int_0^L (PV + \sum_{i=1}^{2} Q_i W_i)dZ, \tag{1}$$

where

$$EI = E_1 I_1 + E_2 I_2 \tag{2}$$

and where $E_i I_i$ and $E_i A_i$ are the bending and the axial stiffnesses of the two beams, P the transversal load per unit length, Q_i the axial loads per unit length, ρA the mass per unit length of the composite. Prime means derivative with respect to the space coordinate $Z \in [0, L]$ and dot derivative with respect to time T. Simple geometric considerations show that

$$S_T = W_1 - W_2 + HV', \tag{3}$$

where H is the distance between the centroids of the two beams. The nonlinear elastic energy stored in the interface per unit length is an even function of S_T,

$$G(S_T, Z) = \frac{K_1(Z)}{2} S_T^2 + \frac{K_3(Z)}{4} S_T^4 + ..., \tag{4}$$

so that the tangential force transmitted through the interface is

$$F_T = \frac{\partial G}{\partial S_T} = K_1(Z) S_T + K_3(Z) S_T^3 + ... \tag{5}$$

The governing equations are obtained by the extended Hamiltonian principle,

$$\delta \int_{T_1}^{T_2} (E_k + E_p - E_s) dT = 0, \tag{6}$$

which provides

$$\begin{aligned} &(EIV'')'' + \rho A \ddot{V} = HF_T' + P, \\ &(E_1 A_1 W_1')' = F_T - Q_1, \\ &(E_2 A_2 W_2')' = -F_T - Q_2, \end{aligned} \tag{7}$$

and the associated b.c. at $Z = 0$ and $Z = L$

$$\begin{aligned} EIV'' = 0 \quad &\text{or} \quad V' = 0, \\ (EIV'')' = HF_T \quad &\text{or} \quad V = 0, \\ E_1 A_1 W_1' = 0 \quad &\text{or} \quad W_1 = 0, \\ E_2 A_2 W_2' = 0 \quad &\text{or} \quad W_2 = 0. \end{aligned} \tag{8}$$

In the previous equations we have that

$$F_T' = \frac{d}{dZ} F_T[S_T(Z,T), Z] = \frac{\partial F_T}{\partial S_T} S_T' + \frac{\partial F_T}{\partial Z}. \tag{9}$$

We assume that the beam is uniform, so that EI, ρA, E_1A_1, E_2A_2 and H are constant, while F_T depends on S_T only, i.e. also the K_i are constants.

It is useful to work with dimensionless equations. Thus, we define

$$\begin{aligned}
&Z = zL, \quad T = tL^2\sqrt{\frac{\rho A}{EI}}, \quad F_T = \frac{EI}{HL^2} f_T, V = Lv,\\
&W_i = \frac{EI}{HE_iA_i} w_i, \quad P = \frac{EI}{L^3} p, \quad Q_i = \frac{EI}{HL^2} q_i,\\
&\frac{1}{EA} = \frac{1}{E_1A_1} + \frac{1}{E_2A_2},\\
&K_i = \left(\frac{EA}{L^2}\right)^i k_i, \qquad \alpha = 1 + H^2\frac{EA}{EI},
\end{aligned} \tag{10}$$

so that eqs. (7) become

$$\begin{aligned}
&v'''' + \ddot{v} = [f_T(S_T)]' + p,\\
&w_1'' = f_T(S_T) - q_1,\\
&w_2'' = -f_T(S_T) - q_2,
\end{aligned} \tag{11}$$

and the associated b.c. at $z = 0$ and $z = 1$ are

$$\begin{aligned}
&v'' = 0 \quad \text{or} \quad v' = 0,\\
&v''' = f_T \quad \text{or} \quad v = 0,\\
&w_1' = 0 \quad \text{or} \quad w_1 = 0,\\
&w_2' = 0 \quad \text{or} \quad w_2 = 0.
\end{aligned} \tag{12}$$

Now prime and dot mean derivatives with respect to $z \in [0,1]$ and t, respectively.

For a two-layer beam made of identical rectangular beams we have $\alpha = 4$. For the steel-concrete beam considered in [10,24] we have $\alpha = 2.78$. These examples show that α is not necessarily close to 1.

The interface slip is given by

$$S_T = \frac{H}{\alpha - 1}\left[\frac{E_2A_2w_1 - E_1A_1w_2}{E_1A_1 + E_2A_2} + (\alpha - 1)\frac{\partial v}{\partial z}\right]. \tag{13}$$

In the following we assume $q_1 = q_2 = 0$. Thus, from $(11)_{2,3}$ we have $(w_1 + w_2)'' = 0$, namely

$$w_2(z,t) = -w_1(z,t) + c_1(t)z + c_2(t), \tag{14}$$

where $c_1(t)$ and $c_2(t)$ are unknown z-independent functions. They are different from zero only for b.c. on w_1 different from those on w_2. From (14) it follows that

$$S_T = H\left(\frac{w_1}{\alpha - 1} + v'\right) - \frac{EI}{H}\frac{c_1(t)z + c_2(t)}{E_2A_2}. \tag{15}$$

Since we are interested in the nonlinear *free* oscillations, we further assume $p = 0$.

In [25] we manipulate the system (11) to obtain a unique sixth order equation. Here we instead proceed with the three coupled equations since they permit an easier handling of b.c.

3 The multiple time scale method

We look for an approximate solution by means of the multiple time scale method [28], so that we assume

$$\begin{aligned}
&v(z,t) = \varepsilon v_1(z,t_0,t_2) + \varepsilon^3 v_3(z,t_0,t_2) + ...,\\
&w_1(z,t) = \varepsilon w_{11}(z,t_0,t_2) + \varepsilon^3 w_{13}(z,t_0,t_2) + ...,\\
&w_2(z,t) = \varepsilon w_{21}(z,t_0,t_2) + \varepsilon^3 w_{23}(z,t_0,t_2) + ...,
\end{aligned} \tag{16}$$

where $t_i = \varepsilon^i t$, i is an integer number, are the slow times and where the missing terms and missing time scales are not considered due to symmetry considerations [25].

By substituting (16) in the equation of motion (11) and in the b.c. (12), by noting that, for example,

$$\frac{\partial^2 v_1}{\partial t^2} = \frac{\partial^2 v_1}{\partial t_0^2} + 2\varepsilon^2\frac{\partial^2 v_1}{\partial t_0 \partial t_2} + ..., \tag{17}$$

and by equating to zero each power of ε, we obtain a sequence of problems which are solved in the following.

4 The first order problem

The first order equations of motion are

$$\begin{aligned}
&\frac{\partial^4 v_1}{\partial z^4} + \frac{\partial^2 v_1}{\partial t_0^2} - k_1\frac{\partial s_{T1}}{\partial z} = 0,\\
&\frac{\partial^2 w_{11}}{\partial z^2} - k_1 s_{T1} = 0,\\
&\frac{\partial^2 w_{21}}{\partial z^2} + k_1 s_{T1} = 0,\\
&s_{T1} = \frac{E_2A_2w_{11} - E_1A_1w_{21}}{E_1A_1 + E_2A_2} + (\alpha - 1)\frac{\partial v_1}{\partial z},
\end{aligned} \tag{18}$$

where s_{T1} is the first order dimensionless interface sliding,

$$S_T = \frac{H}{(\alpha - 1)}(\varepsilon s_{T1} + ...) \tag{19}$$

(see eq. (13)). Since we are looking for nonlinear oscillations, a solution of (18) is sought-after in the form

$$\begin{aligned}
&v_1(z,t_0,t_2) = g(t_0,t_2)f_1(z),\\
&w_{11}(z,t_0,t_2) = g(t_0,t_2)f_2(z),\\
&w_{21}(z,t_0,t_2) = g(t_0,t_2)f_3(z),\\
&g(t_0,t_2) = A_c(t_2)\cos(\omega t_0) + A_s(t_2)\sin(\omega t_0),
\end{aligned} \tag{20}$$

so that (18) becomes

$$\begin{aligned}
&f_1'''' - \omega^2 f_1 - k_1 f_4' = 0,\\
&f_2'' - k_1 f_4 = 0,\\
&f_3'' + k_1 f_4 = 0,\\
&f_4 = \frac{E_2A_2f_2 - E_1A_1f_3}{E_1A_1 + E_2A_2} + (\alpha - 1)f_1'.
\end{aligned} \tag{21}$$

Note that

$$s_{T1} = g(t_0,t_2)f_4(z). \tag{22}$$

The general solution of (21) is given by

$$f_1(z) = \sum_{i=1}^{6} j_i e^{l_i z},$$
$$f_2(z) = E_1A_1(j_7 z + j_8) + k_1(\alpha - 1)\sum_{i=1}^{6} \frac{l_i}{l_i^2 - k_1} j_i e^{l_i z},$$
$$f_3(z) = E_2A_2(j_7 z + j_8) - k_1(\alpha - 1)\sum_{i=1}^{6} \frac{l_i}{l_i^2 - k_1} j_i e^{l_i z}, \tag{23}$$

where the l_i are the six roots of

$$l^6 - k_1\alpha l^4 - \omega^2 l^2 + k_1\omega^2 = 0. \tag{24}$$

Actually, (24) is a third order algebraic equation in $m = \sqrt{l}$, so that the solution is known in closed form. The j_i are the eight constants of integrations that, together with the first order (linear) circular frequency ω, are determined by the b.c. and by the normalization condition.

The adjoint equations of (21) are

$$F_1'''' - \omega^2 F_1 + k_1(\alpha - 1)F_4' = 0,$$
$$F_2'' - k_1 \frac{E_2A_2}{E_1A_1 + E_2A_2} F_4 = 0,$$
$$F_3'' + k_1 \frac{E_1A_1}{E_1A_1 + E_2A_2} F_4 = 0,$$
$$F_4 = F_2 - F_3 - F_1'. \tag{25}$$

The solution of the adjoint equations will be required in the following in the solvability condition. By comparing eqs. (21) and (25), and the associated b.c. (see the next Sect. 4.1), it is possible to see that

$$F_1(z) = f_1(z),$$
$$F_2(z) = -\frac{E_2A_2}{E_1A_1 + E_2A_2}\frac{1}{\alpha - 1} f_2(z),$$
$$F_3(z) = -\frac{E_1A_1}{E_1A_1 + E_2A_2}\frac{1}{\alpha - 1} f_3(z),$$
$$F_4(z) = -\frac{1}{\alpha - 1} f_4(z), \tag{26}$$

so that the solution of the adjoint problem can be easily obtained from that of the original problem.

4.1 Boundary conditions

At a *free* boundary ($z = 0$ and/or $z = 1$) we have

$$f_1'' = 0, \;\; f_1''' - k_1 f_4 = 0, \;\; f_2' = 0, \;\; f_3' = 0, \tag{27}$$

while the b.c. of the adjont equations are

$$F_1'' = 0, \;\; F_1''' + k_1(\alpha - 1)F_4 = 0, \;\; F_2' = 0, \;\; F_3' = 0. \tag{28}$$

At a *fixed* boundary we have

$$f_1 = 0, \;\; f_1' = 0, \;\; f_2 = 0, \;\; f_3 = 0,$$
$$F_1 = 0, \;\; F_1' = 0, \;\; F_2 = 0, \;\; F_3 = 0. \tag{29}$$

At a *hinged* boundary we have

$$f_1 = 0, \;\; f_1'' = 0, \;\; f_2' = 0, \;\; f_3' = 0,$$
$$F_1 = 0, \;\; F_1'' = 0, \;\; F_2' = 0, \;\; F_3' = 0. \tag{30}$$

Finally, if the layer 1 is fixed and the layer 2 is free we have

$$f_1 = 0, \;\; f_1' = 0, \;\; f_2 = 0, \;\; f_3' = 0,$$
$$F_1 = 0, \;\; F_1' = 0, \;\; F_2 = 0, \;\; F_3' = 0. \tag{31}$$

4.2 Linear natural frequency

The (linear) circular frequency ω is a function of the parameters α and k_1; when the two layers have different b.c. on the same side (see eqs. (31)), it also depends on the ratio E_1A_1/E_2A_2, since in this case $c_1(t)$ or $c_2(t)$ are different from zero (see eq. (15)), i.e. $j_7 \neq 0$ or $j_8 \neq 0$ (see eq. (23)).

Before to proceed we remark that we are interested only in (mainly) flexural vibrations, so we do not consider the linear frequencies associated to (mainly) longitudinal vibrations, which actually can be detected by the considered formulas. Furthermore, we limit our analysis to the first three frequencies because for high order frequencies equations (7) are not expected to accurately describe the real behaviour.

Symmetric b.c. As representative cases of symmetric (with respect to $z = 1/2$) b.c. we consider the fixed-fixed constraints. This choice is due to the lack of space, although we have the results for others b.c.; in particular, we have found that the curves for the free-free case (which are reported in [25] for the first natural frequency) are very close to those of the fixed-fixed case.

The first three natural frequencies $\omega(\alpha)$ for different values of k_1 are reported in Fig. 1.

Unsymmetric b.c. As representative cases of unsymmetric b.c. we consider the fixed-free constraints. The first three natural frequencies $\omega(\alpha)$ for different values of k_1 are reported in Fig. 2.

B.c. different on each layer. As representative cases of (symmetric, indeed) b.c. different on each layer we consider the case in which the layer 1 is fixed-fixed and the layer 2 is free-free. The first three natural frequencies $\omega(\alpha)$ for different values of k_1 and for different values of the ratio E_1A_1/E_2A_2 are reported in Fig. 3. Note that the second frequency does *not* depend on E_1A_1/E_2A_2, while for the first and the third frequencies the differences due to E_1A_1/E_2A_2 are visible only for $k_1 = 10$ and $k_1 = 100$.

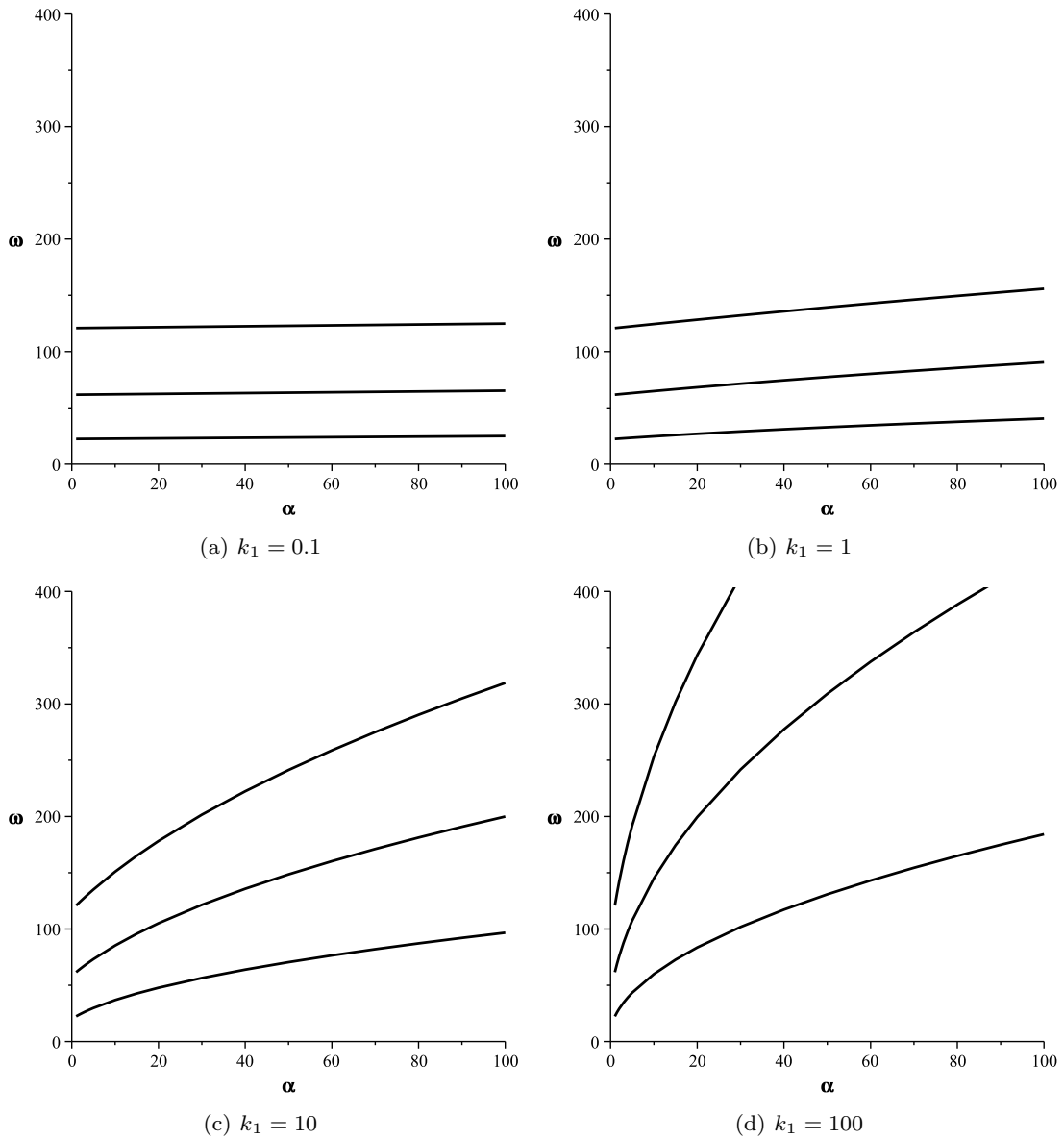

(a) $k_1 = 0.1$ (b) $k_1 = 1$

(c) $k_1 = 10$ (d) $k_1 = 100$

Fig. 1 The first three natural frequencies ω for fixed-fixed b.c.

Comparing Figs. 1-3 we see the stiffening effect of both the parameters α and k_1, since ω is an increasing functions of α and k_1, starting from $\omega_{\text{lim}} = \omega(\alpha = 1) = \omega(k_1 = 0)$ (see Sect. 4.3) and approaching infinity for both $\alpha \to \infty$ and $k_1 \to \infty$.

It is worth to note that moving far from $\alpha = 1$ and $k_1 = 0$ the values of the frequencies strongly increase, so that the asymptotic approximations reported in Sect. 4.3 are inadequate for almost all values of the parameters and the full analysis is actually required.

The family of curves for different b.c. share the same qualitative behavior, so we can conclude that the effect of the b.c. is mainly quantitative. In fact, for fixed values of α and k_1 we have very different natural frequencies for different b.c., much more different of what happens for the single beam. In other words, the b.c. affect the two-layer beam much more that what they do for a single beam.

4.3 Limit cases

In this section we study the asymptotic behaviour of ω for limit values of the main parameters α and k_1.

a) $k_1 \to 0$. For $k_1 = 0$ eqs. (21) decouple, so that the solution ω_{lim} (i) does not depend on α and (ii) it is that

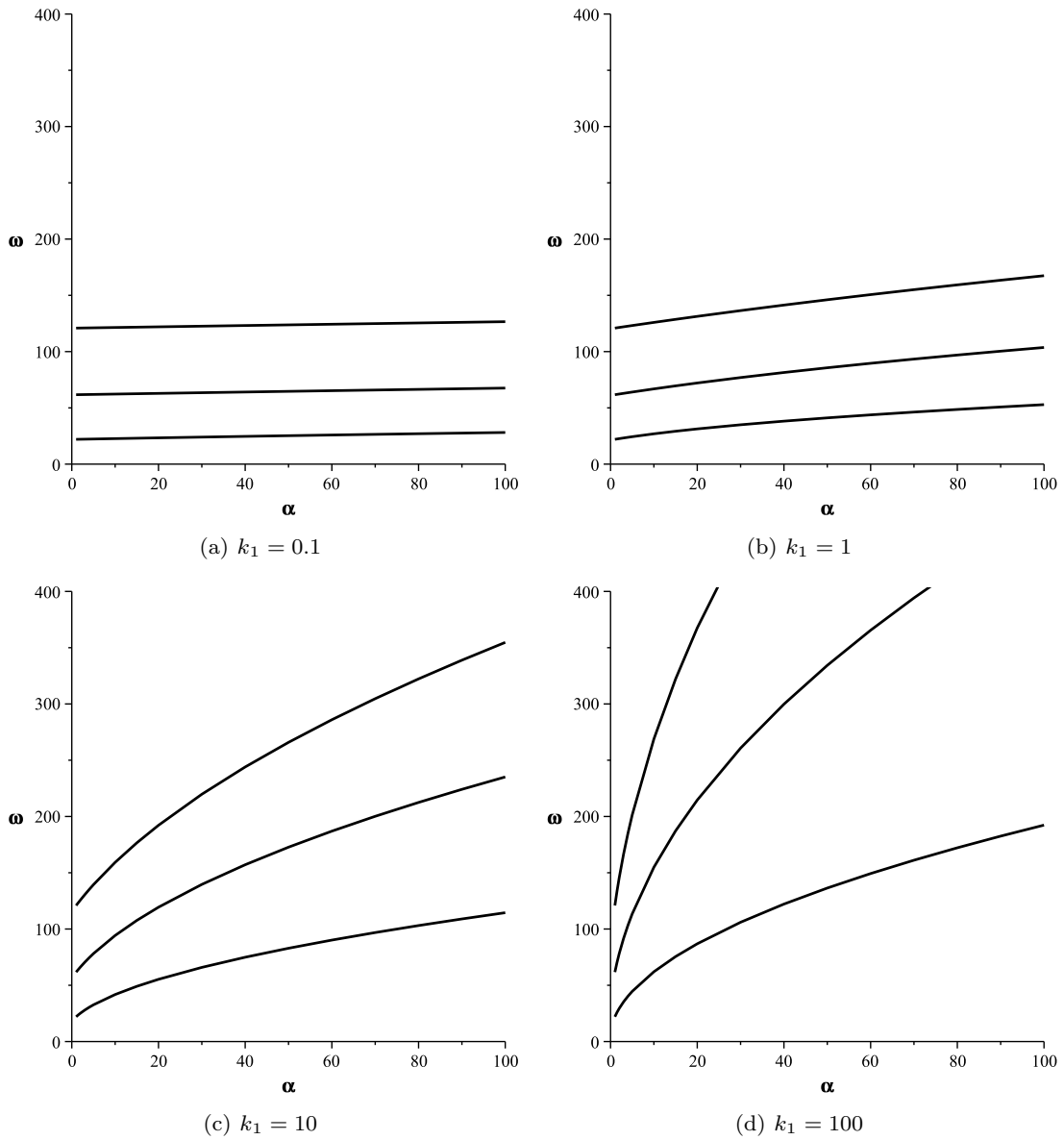

(a) $k_1 = 0.1$ (b) $k_1 = 1$

(c) $k_1 = 10$ (d) $k_1 = 100$

Fig. 2 The first three natural frequencies ω for fixed-free b.c.

of a single equivalent beam of bending stiffness EI, and can be computed easily. It is the solution of the limit equations reported in Tab. 1.

By performing a straightforward analysis it is possible to show that for small values of k_1 we have the following asymptotic behaviour

$$\omega = \omega_{\text{lim}} + k_1(\alpha - 1)\omega_1 + o(k_1). \tag{32}$$

The values of ω_{lim} and of ω_1 are reported in Tab. 2 for the first natural frequencies. Note that the fixed-fixed and the fixed-fixed/free-free cases have the same asymptotic development. Furthermore, in the latter case there is no dependency on the ratio E_1A_1/E_2A_2, which will appear at higher k_1-orders (see Fig. 3).

Table 1 The limit equations for determining ω_{lim}.

b.c.	limit equation
free-free	$\cos(\sqrt{\omega_{\text{lim}}})\cosh(\sqrt{\omega_{\text{lim}}}) = 1$
fixed-fixed	$\cos(\sqrt{\omega_{\text{lim}}})\cosh(\sqrt{\omega_{\text{lim}}}) = 1$
fixed-free	$\cos(\sqrt{\omega_{\text{lim}}})\cosh(\sqrt{\omega_{\text{lim}}}) = -1$
fixed-hinged	$\tan(\sqrt{\omega_{\text{lim}}}) = \tanh(\sqrt{\omega_{\text{lim}}})$
hinged-hinged	$\sin(\sqrt{\omega_{\text{lim}}}) = 0$
fixed-fixed/free-free	$\cos(\sqrt{\omega_{\text{lim}}})\cosh(\sqrt{\omega_{\text{lim}}}) = 1$

b) $\alpha \to 1$. Another pathological situation occurs for $\alpha = 1$. Now f_4 no longer depends on f_1 (see eq. (21)), so that again the equations decouple and the flexural

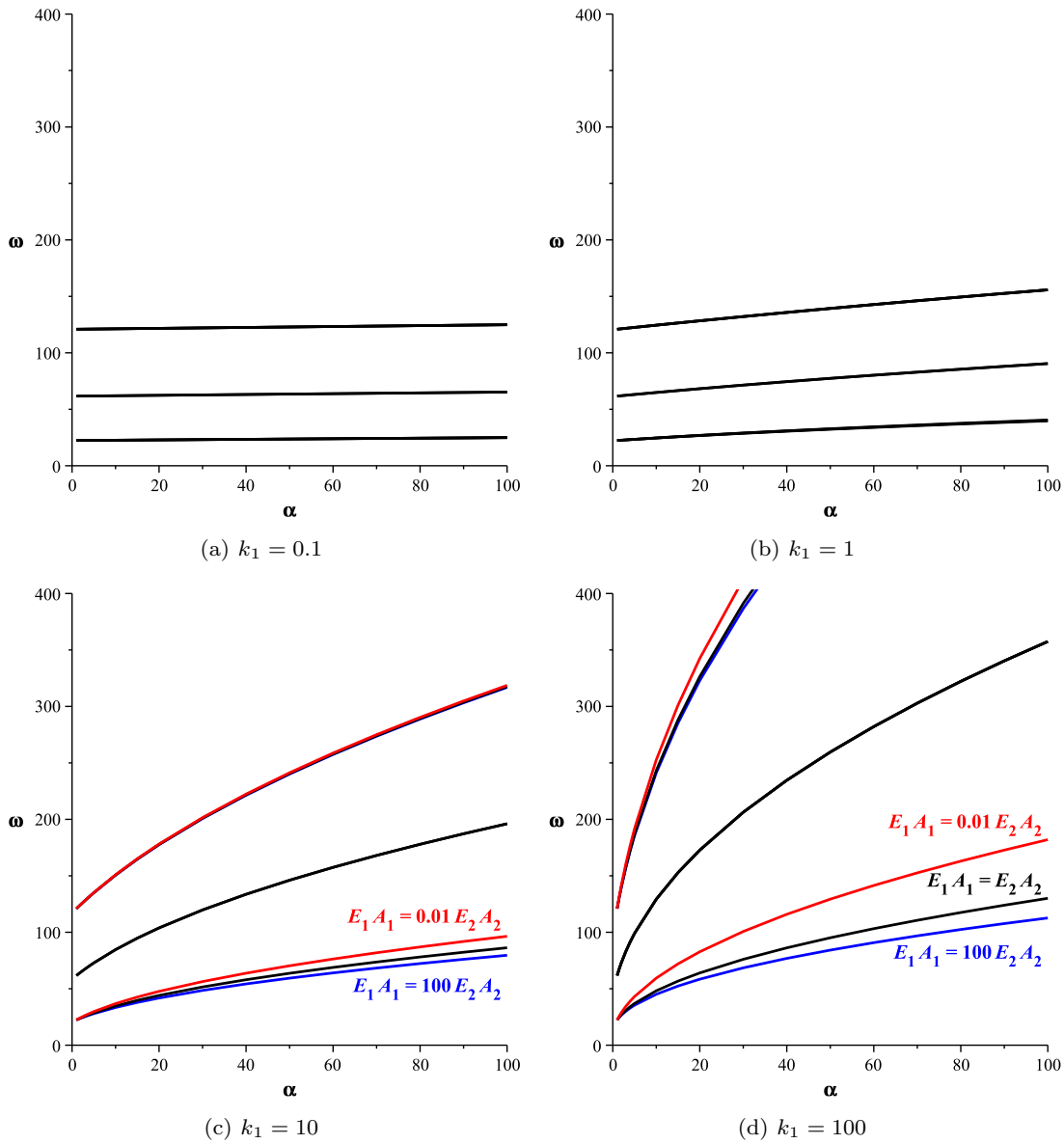

(a) $k_1 = 0.1$ (b) $k_1 = 1$

(c) $k_1 = 10$ (d) $k_1 = 100$

Fig. 3 The first three natural frequencies ω for fixed-fixed/free-free b.c. For each value of $n = 1$ and of $n = 3$ we have three curves: the upper is for $E_1A_1 = 0.01E_2A_2$, the medium for $E_1A_1 = E_2A_2$ and the lower for $E_1A_1 = 100E_2A_2$

natural frequencies become independent of k_1 and equal to the ω_{lim} previously reported.

c) $k_1 \to \infty$ *and* $\alpha \to \infty$. In these limit cases we note the occurrence of the boundary layer phenomenon, where the deformation tends to localize near the boundaries. Mathematically, this is due to the singular nature of the perturbation; in fact, it is easy to see that when $k_1 \to \infty$ and $\alpha \to \infty$, respectively, equation (24) reduces the order from 6 to 4 and from 6 to 2. Alternatively, this can be seen by noting that one root l of (24) behaves like $l \simeq k_1\alpha$, i.e. it goes to infinity, for *both* $k_1 \to \infty$ and $\alpha \to \infty$.

An example is illustrated in Fig. 4, where we see how the dimensionless interface sliding f_4 (see eq. (22)) accumulates on 1 near $z = 0$ for increasing values of α. Note that the normalization condition (40) is satisfied.

5 The third order problem

The solution of the third order equations is sought-after in the form

$$v_3(z, t_0, t_2) = v_{3c}(z)\cos(\omega t_0) + v_{3s}(z)\sin(\omega t_0) + v_{3c3}(z)\cos(3\omega t_0) + v_{3s3}(z)\sin(3\omega t_0),$$

Table 2 The first values of $\omega_{\lim}$ and ω_1.

b.c.	n	$\omega_{\lim}$	ω_1
free-free	1	22.3733	1.1058
	2	61.6728	0.8831
	3	120.9034	0.7728
fixed-fixed	1	22.3733	0.2749
	2	61.6728	0.3733
	3	120.9034	0.4090
fixed-free	1	3.5160	0.6609
	2	22.0345	0.7356
	3	61.6972	0.6264
	4	120.9019	0.5910
fixed-hinged	1	15.4182	0.3733
	2	49.9649	0.4293
	3	104.2477	0.4510
hinged-hinged	1	π^2	0.5
	2	$4\pi^2$	0.5
	3	$9\pi^2$	0.5
fixed-fixed/free-free	1	22.3733	0.2749
	2	61.6728	0.3733
	3	120.9034	0.4090

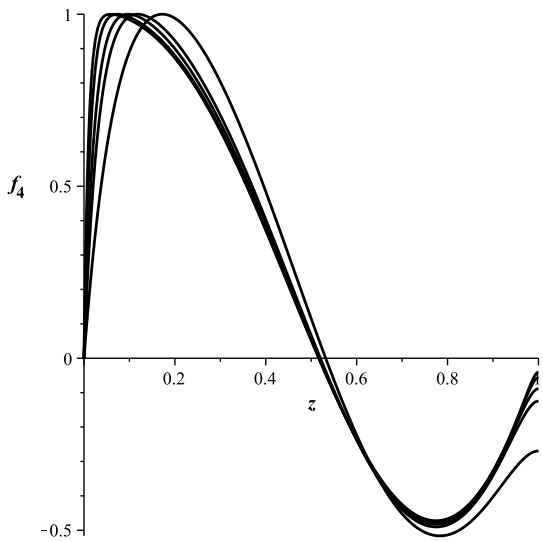

Fig. 4 The boundary layer phenomenon for fixed-free b.c. $k_1 = 100$ and $\alpha = 100; 50; 20; 10; 2$ (from the left to the right)

$$\begin{aligned} w_{13}(z,t_0,t_2) &= w_{13c}(z)\cos(\omega t_0) + w_{13s}(z)\sin(\omega t_0) \\ &\quad + w_{13c3}(z)\cos(3\omega t_0) + w_{13s3}(z)\sin(3\omega t_0), \\ w_{23}(z,t_0,t_2) &= w_{23c}(z)\cos(\omega t_0) + w_{23s}(z)\sin(\omega t_0) \\ &\quad + w_{23c3}(z)\cos(3\omega t_0) + w_{23s3}(z)\sin(3\omega t_0). \end{aligned} \tag{33}$$

This is suggested by the cubic nonlinearities, by the expression $[\cos(t)]^3 = [3\cos(t) + \cos(3t)]/4$ and by similar expressions.

The equations for v_{3c}, w_{13c} and w_{23c} are

$$\begin{aligned} & v_{3c}'''' - \omega^2 v_{3c} - k_1 s_{T3c}' = -2\omega f_1 \frac{\partial A_s}{\partial t_2} \\ & + k_3 A_c (A_c^2 + A_s^2) \frac{3EI^2}{4H^2L^6} (f_4^3)', \\ & w_{13c}'' - k_1 s_{T3c} = k_3 A_c (A_c^2 + A_s^2) \frac{3EI^2}{4H^2L^6} (f_4^3), \\ & w_{23c}'' + k_1 s_{T3c} = -k_3 A_c (A_c^2 + A_s^2) \frac{3EI^2}{4H^2L^6} (f_4^3), \\ & s_{T3c} = \frac{E_2 A_2 w_{13c} - E_1 A_1 w_{23c}}{E_1 A_1 + E_2 A_2} + (\alpha - 1) v_{3c}'. \end{aligned} \tag{34}$$

We see that this is the non-homogenous version of the problem (21), so that the solution exists if and only if the solvability condition is satisfied. For every b.c. this latter is given by

$$\begin{aligned} & -2\omega \frac{\partial A_s}{\partial t_2} \int_0^1 f_1 F_1 dz \\ & + k_3 A_c (A_c^2 + A_s^2) \frac{3EI^2}{4H^2L^6} \int_0^1 f_4^3 F_4 dz = 0. \end{aligned} \tag{35}$$

The equations for v_{3s}, w_{13s} and w_{23s} are instead

$$\begin{aligned} & v_{3s}'''' - \omega^2 v_{3s} - k_1 s_{T3s}' = 2\omega f_1 \frac{\partial A_s}{\partial t_2} \\ & + k_3 A_s (A_c^2 + A_s^2) \frac{3EI^2}{4H^2L^6} (f_4^3)', \\ & w_{13s}'' - k_1 s_{T3s} = k_3 A_s (A_c^2 + A_s^2) \frac{3EI^2}{4H^2L^6} (f_4^3), \\ & w_{23s}'' + k_1 s_{T3c} = -k_3 A_s (A_c^2 + A_s^2) \frac{3EI^2}{4H^2L^6} (f_4^3), \\ & s_{T3s} = \frac{E_2 A_2 w_{13s} - E_1 A_1 w_{23s}}{E_1 A_1 + E_2 A_2} + (\alpha - 1) v_{3s}', \end{aligned} \tag{36}$$

and the solvability condition is, for every b.c.,

$$\begin{aligned} & 2\omega \frac{\partial A_c}{\partial t_2} \int_0^1 f_1 F_1 dz \\ & + k_3 A_s (A_c^2 + A_s^2) \frac{3EI^2}{4H^2L^6} \int_0^1 f_4^3 F_4 dz = 0. \end{aligned} \tag{37}$$

Rearranging the two solvability conditions, we get

$$\begin{aligned} & \frac{\partial A_s}{\partial t_2} + k_3 \frac{3EI^2}{4H^2L^6} \eta A_c (A_c^2 + A_s^2) = 0, \\ & \frac{\partial A_c}{\partial t_2} - k_3 \frac{3EI^2}{4H^2L^6} \eta A_s (A_c^2 + A_s^2) = 0, \end{aligned} \tag{38}$$

which permits us to determine $A_c(t_2)$ and $A_s(t_2)$. In (38) the major role is played by the *positive* nonlinearity parameter

$$\eta = -\frac{3}{8\omega} \frac{\int_0^1 f_4^3 F_4 dz}{\int_0^1 f_1 F_1 dz} = \frac{3}{8\omega(\alpha - 1)} \frac{\int_0^1 f_4^4 dz}{\int_0^1 f_1^2 dz} \tag{39}$$

which is the *same* parameter used in [25] (see eq. (57) of [25], where a different but equivalent expression is reported).

Note that η depends on the amplitude of the f_i, so that their normalization is important. We assume

$$\max\{f_4(z)\} = 1. \tag{40}$$

Other normalizations are possible and, as the considered one, make sense from an engineering point of view, for example $\max\{f_1(z)\} = 1$; note however that all normalizations are theoretically equivalent, since there is a one-to-one map between them. We choose (40) because it is the same used in [25], so that we can directly compare the present results with those reported in [25]; its mechanical motivation is illustrated in next eq. (44).

The coefficient η depends on α, k_1 and, for some b.c., also on the ratio E_1A_1/E_2A_2; for different b.c. it is reported in Figs. 5, 6 and 7, where we see that it is an increasing function of α but, contrarily to ω, it is a decreasing function of k_1, rapidly approaching 0 for $k_1 \to \infty$. We also have $\eta = 0$ for $\alpha = 1$, a fact that is counter-intuitive if one looks at eq. (39), but that can be proved by noting that f_4 rapidly converge to 0 for $\alpha \to 1$.

A stationary solution of (38) is given by

$$\begin{aligned} A_c &= \Gamma \cos(\Omega t_2), \\ A_s &= \Gamma \sin(\Omega t_2), \end{aligned} \tag{41}$$

where

$$\Omega = -k_3 \frac{EI^2}{H^2L^6}\eta\Gamma^2. \tag{42}$$

It follows that

$$\begin{aligned} &g(t_0, t2) = A_c \cos(\omega t_0) + A_s \sin(\omega t_0) = \\ &\Gamma[\cos(\Omega t_2)\cos(\omega t_0) + \sin(\Omega t_2)\sin(\omega t_0)] = \\ &\Gamma \cos(\omega t_0 - \Omega t_2) = \\ &\Gamma \cos\left[\left(\omega + k_3 \frac{EI^2}{H^2L^6}\eta\varepsilon^2\Gamma^2\right)t\right]. \end{aligned} \tag{43}$$

From (13), using (18), (22) and the normalization condition (40), we conclude that

$$A = \max\{S_T\} = \frac{H}{\alpha - 1}\varepsilon\Gamma + ... \tag{44}$$

is the amplitude of the real interface sliding. This is worthy, since it is just in the interface sliding that we have the nonlinearities, so that the chosen amplitude is that directly connected to the nonlinear behavior of the system. If we chose a normalization different from (40), we lose this property.

From the previous developments we conclude that the nonlinear, amplitude depend, frequency is given by

$$\omega_{nl} = \omega + k_3 \frac{EI^2(\alpha - 1)^2}{H^4L^6}\eta A^2. \tag{45}$$

The physical natural frequency is then

$$f_{nl} = \frac{1}{2\pi L^2}\sqrt{\frac{EI}{\rho A}}\left(\omega + \frac{K_3}{EA}\eta A^2\right). \tag{46}$$

The major role in determining the backbone curve (45), and its dimensional version (46), is played by the parameter η, which is reported in Figs. 5-7. The fact that it is always positive means, as expected, that an hardening ($k_3 > 0$) / softening ($k_3 < 0$) behaviour of the interface corresponds an hardening / softening behaviour of the whole structure.

6 Conclusions

The nonlinear dynamics of a two-layer beam made of two linear elastic Euler-Bernoulli beams and by a nonlinear elastic interface have been investigated by means of the multiple time scale method. The effects of different b.c., symmetric and not symmetric, equal on each layer or different for the two layers, have been studied.

The natural linear frequencies are computed first, and it is shown that they depend on two dimensionless parameters only if the b.c. are the same on each layer. Otherwise, they also depend on the ratio E_1A_1/E_2A_2 of the beams axial stiffenesses. It is shown that the linear natural frequencies have a weak *qualitative* dependence and a strong *quantitative* dependence on the different b.c., much more strong of what happens for a single beam.

The amplitude dependent corrections of the linear natural frequencies, which is the main effect of the problem nonlinearity, have been successively computed. It is found that the hardening/softening behavior of the interface is maintained in the whole structure. Again, the effects of the different boundary condition have been highlighted to be mainly of quantitative nature, so that in applications one must pay a lot of attention to their determination.

The multiple time scale method is found to be a useful mathematical tool for analytical, although approximate, computation of the effects on the nonlinearity in the free vibrations of complex composite beams.

Acknowledgements This work has been partially supported by the Italian Ministry of Education, University and Research (MIUR) by the PRIN funded program 2010/11 N.2010MBJK5B "Dynamics, stability and control of flexible structures".

A preliminary version of this work is presented in [29].

References

1. Yu Y-Y (1962) Nonlinear flexural vibrations of sandwich plates. J Acous Soc America 34(9A): 1176–1183
2. Sorge F (1995) On the flexural vibrations of sandwich plates. Meccanica 30:397–403
3. Sokolinsky VS, von Bremen HF, Lavoie JA, Nutt SR (2004) Analytical and experimental study of free vibration response of soft-core sandwich beams. J Sandwich Struct Mater 6:239–261

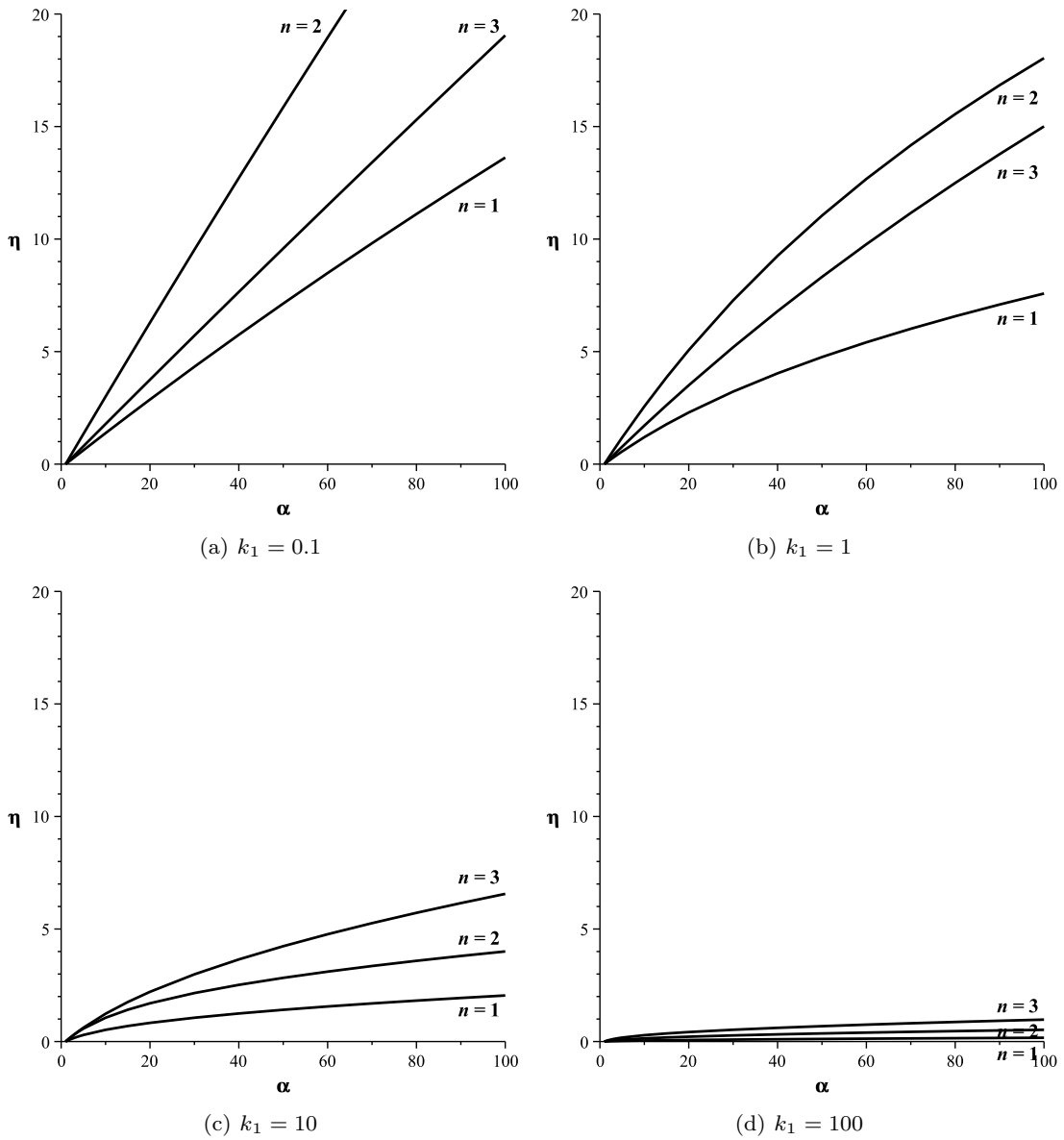

(a) $k_1 = 0.1$ (b) $k_1 = 1$

(c) $k_1 = 10$ (d) $k_1 = 100$

Fig. 5 The nonlinear coefficient η for fixed-fixed b.c.

4. Howson WP, Zare A (2005) Exact dynamic stiffness matrix for flexural vibration of three-layered sandwich beams. J Sound Vibr 282:753–767
5. Chakrabarti A, Rasajit Kumar Bera (2006) Large amplitude vibration of thin homogeneous heated orthotropic sandwich elliptic plates. J Ther Stress 29:21–36
6. Arvin H, Sadighi M, Ohadi AR (2010) A numerical study of free and forced vibration of composite sandwich beam with viscoelastic core. Comp Struct 92:996–1008
7. Ivanov IV, Velchev DS, Sadowski T, Kneć M. (2011) Computational models of laminated glass plate under transverse static loading. In: Altenbach H, Eremeyev V (eds.) Shell-Like Structures Non-classical Theories and Applications. Advanced Structured Materials, Springer, Berlin, vol. 15, pp. 469–490. doi:10.1007/978-3-642-21855-2
8. Youzera H, Meftah SA, Challamel N, Tounsi A (2012) Nonlinear damping and forced vibration analysis of laminated composite beams. Composites Part B, 43:1147–1154
9. Challamel N (2012) On geometrically exact post-buckling of composite columns with interlayer slip - The partially composite elastica. Int J Nonlinear Mech 47:7-17
10. Dilena, M, Morassi A (2003) A damage analysis of steel-concrete composite beams via dynamic methods. Part II: analytical models and damage detection. J Vibr Control 9:529–565
11. He X (2005) The nonlinear behaviors of a symmetric isotropic laminate in a mixed boundary condition subject to an arbitrary thermal field coupled with mechanical loading. ASME J Comp Nonlinear Dyn 1:168–177
12. Tanveer M, Singh AV (2009) Linear and nonlinear dynamic responses of various shaped laminated composite plates. ASME J Comp Nonlinear Dyn 4:041011-1–13
13. Jun L, Hongxing H (2011) Free vibration analyses of axially loaded laminated composite beams based on higher-

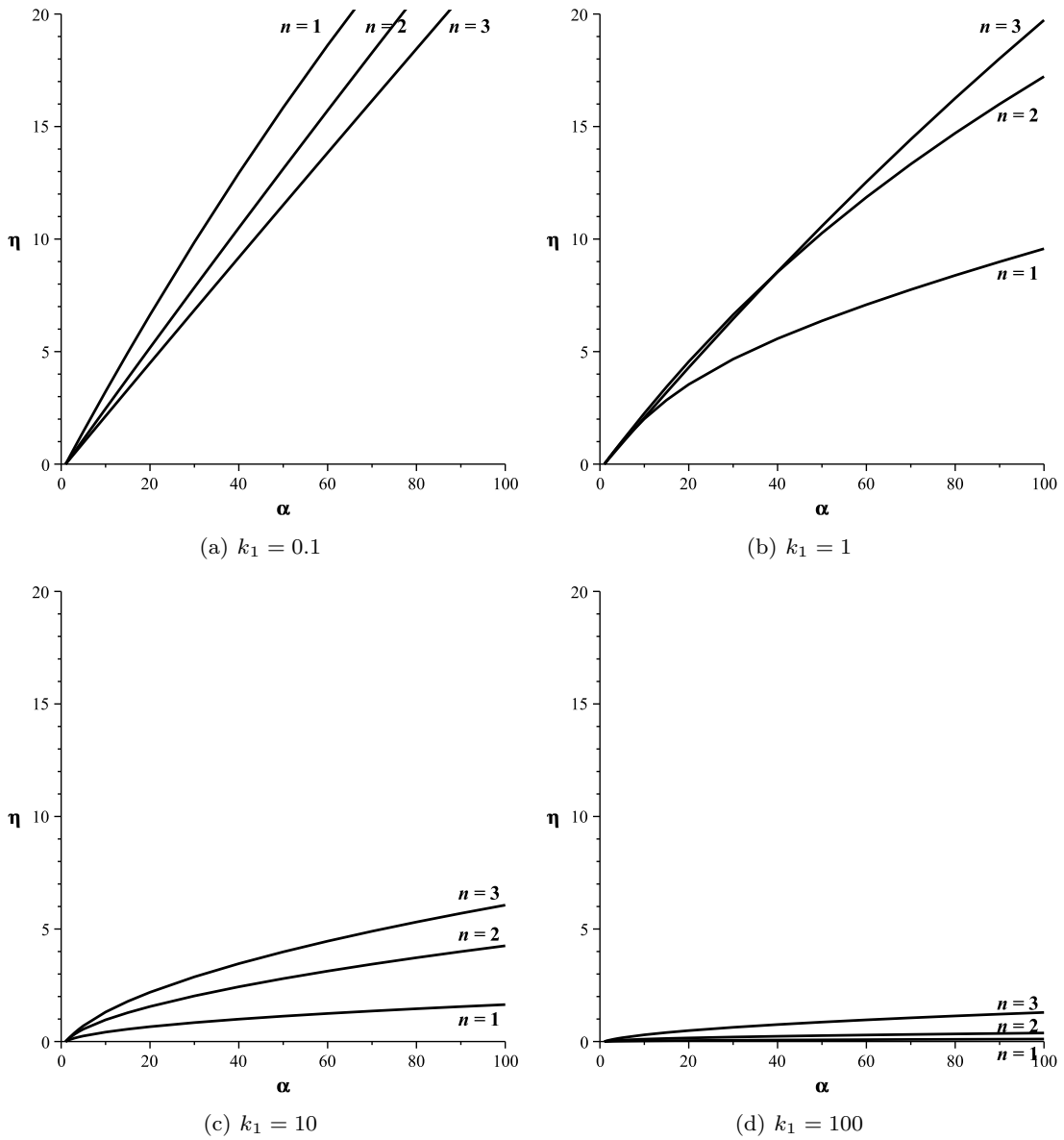

(a) $k_1 = 0.1$ (b) $k_1 = 1$

(c) $k_1 = 10$ (d) $k_1 = 100$

Fig. 6 The nonlinear coefficient η for fixed-free b.c.

order shear deformation theory. Meccanica 46:1299–1317
14. Dai L, Sun L (2012) On the fuzzy sliding mode control of nonlinear motions in a laminated beam. J Appl Nonlinear Dyn 1:287–307
15. Nguyen Q-H, Hjiaj M, Le Grognec P (2012) Analytical approach for free vibration analysis of two-layer Timoshenko beams with interlayer slip. J Sound Vibr 331:2949–2961
16. Lenci S, Clementi F (2012) Effects of shear stiffness, rotatory and axial inertia, and interface stiffness on free vibrations of a two-layer beam. J Sound Vibr 331:5247–5267
17. Lenci S, Rega G (2013) An asymptotic model for the free vibrations of a two-layer beam. Eur J Mech A/Solids 42:441–453
18. Subramanian P (2006) Dynamic analysis of laminated composite beams using higher order theories and finite elements. Comp Struct 73:342–353
19. Arvin H, Sadighi M, Ohadi AR (2010) A numerical study of free and forced vibration of composite sandwich beam with viscoelastic core. Comp Struct 92:996–1008
20. Krishnaswamy S, Chandrashekhara K, Wu WZ (1992) Analytical solutions to vibration of generally layered composite beams. J Sound Vibr 159:85–99
21. Khdeir AA, Reddy JN (1994) Free vibration of cross-ply laminated beams with arbitrary boundary conditions. Int J Eng Sci 32:1971–1980
22. Lenci S, Clementi F (2012) On flexural vibrations of shear deformable laminated beams. In ASME International Mechanical Engineering Congress and Exposition (IMECE 2012), Houston, Texas, USA, 9-15 November 2012, paper n. IMECE 2012-86617.
23. Aly MF, Goda IGM, Hassan GA (2010) Experimental investigation of the dynamic characteristics of laminated composite beams. Int J Mech Mechatr Eng 10:59–68

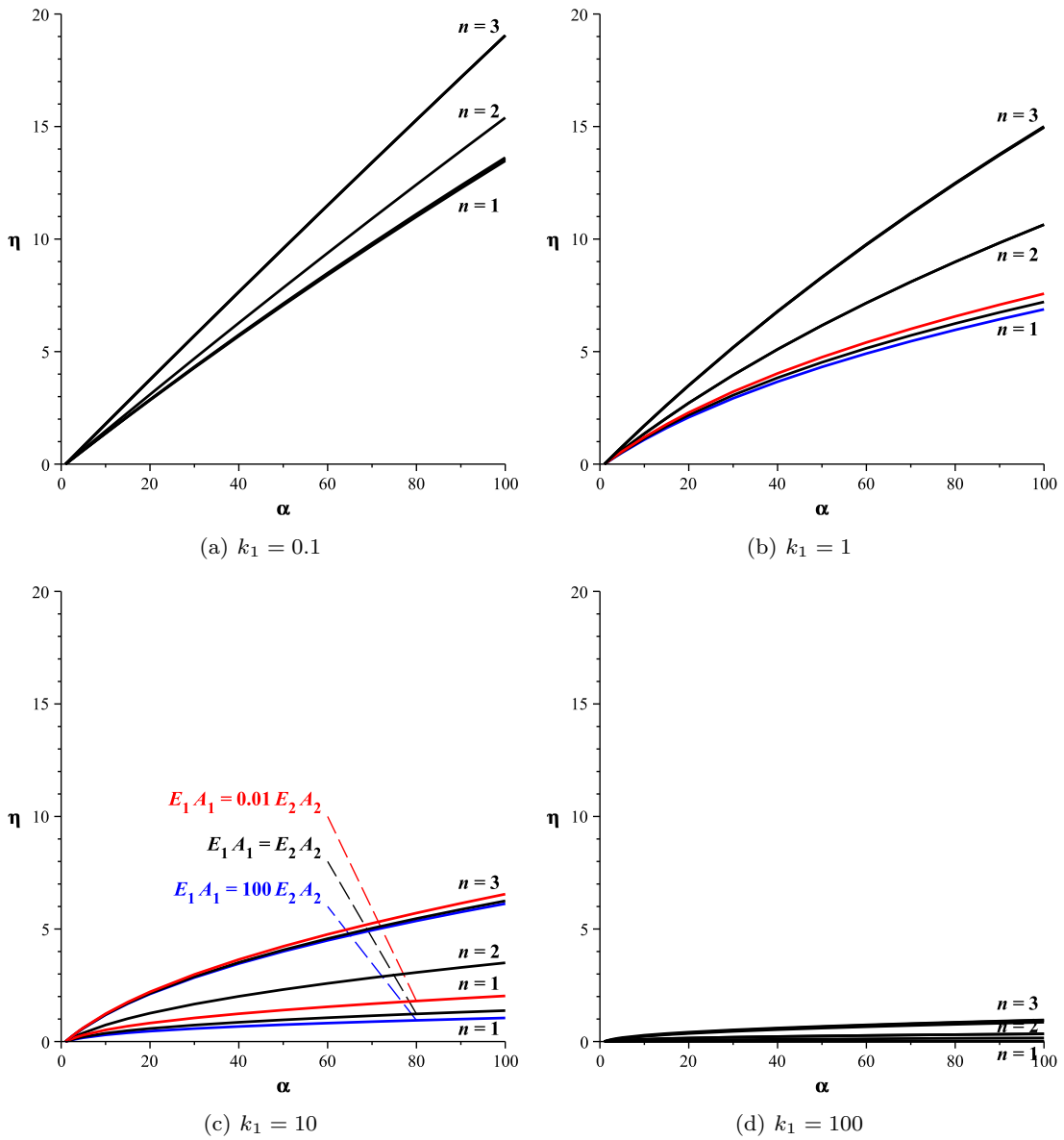

(a) $k_1 = 0.1$ (b) $k_1 = 1$

(c) $k_1 = 10$ (d) $k_1 = 100$

Fig. 7 The nonlinear coefficient η for fixed-fixed/free-free b.c. For each value of $n = 1$ and of $n = 3$ we have three curves: the upper is for $E_1A_1 = 0.01E_2A_2$, the medium for $E_1A_1 = E_2A_2$ and the lower for $E_1A_1 = 100E_2A_2$.

24. Dilena M, Morassi A (2004) Experimental modal analysis of steel-concrete composite beams with partially damaged connection. J Vibr Control 10:897–913

25. Lenci S, Warminski J (2012) Free and forced nonlinear oscillations of a two-layer composite beam with interface slip. Nonlinear Dyn 70:2071–2087

26. Wei H, Kong X (2010) Effect of non-linear in-plane honeycomb core modulus on forced vibration of sandwich beam. In Proc. of ISSCAA2010: 3rd International Symposium on Systems and Control in Aeronautics and Astronautics, Harbin, China, 8-10 June, pp. 478-482. ISBN:978-142446044-1, doi:10.1109/ISSCAA.2010.5632499

27. Faella C, Martinelli E, Nigro E (2003) Shear connection nonlinearity and deflections of steel-concrete composite beams: a simplified method. ASCE J Struct Eng 129:12–20

28. Nayfeh AH, Mook DT (1979) Nonlinear oscillations. Wiley

29. Clementi F, Warminski J, Lenci S (2013) Nonlinear dynamics of a two-layer composite beam with nonlinear interface. In: Proc. of 21th AIMETA Congress of Theoretical and Applied Mechanics, Turin, 17-20 September 2013, ISBN: 978-88-8239-183-6.